
**ELECTRODYNAMICS
AND WAVE PROPAGATION**

Numerical Electrodynamics Analysis of the Interior Problem for a Huygens Element That Is an Interior Huygens Cube

A. S. Godin^a, A. B. Tsai^b, and K. N. Klimov^a

^a*Lianozovo Electromechanical Plant (Research and Production Corporation)*,
Dmitrovskoe shosse 110, Moscow, 127411 Russia

^b*Morinformсистема-Agat Concern, Shosse Entuziastov 29, Moscow, 105275 Russia*
e-mail: andrey.godin@gmail.com, const0@mail.ru

Received June 25, 2014

Abstract—A numerical solution to an electrodynamic problem obtained with the use of the ANSYS HFSS v. 15 code is compared with a known analytic solution. It is shown that, with an increase in frequency, the accuracy of the numerical solution degrades in both the amplitude and the phase.

DOI: 10.1134/S1064226915020059

1. ANALYSIS OF THE HUYGENS CUBE

We consider cube A with the dimensions of $1 \times 1 \times 1$ mm (Fig. 1). Cube A is filled with vacuum. Tangential electric field E_τ on faces 1 and 2 of cube A (Fig. 2) is set equal to zero, which corresponds to a metallic wall. Faces 1 and 2 of this cube are assumed to be short-circuited [1–3].

On faces 3 and 4 of the cube A (Fig. 2), we set the tangential magnetic field H_τ equal to zero, which corresponds to a magnetic wall. Faces 3 and 4 of this cube are assumed to be open-circuited [1–3].

On faces 5 and 6 of the cube A (Figs. 4, 5), we impose the boundary conditions corresponding to the excitation and matching of plane waves [1–3]. The polarizations of the electric and magnetic fields and the directions of the Poynting vectors of these plane waves are shown in Figs. 6–8.

The geometry of the vacuum cube A with the above-introduced boundary conditions will be called the interior Huygens cube. By analogy with the Huygens element [4–6], this definition can be extended as follows: an infinitesimal cube simulating the front of a linearly polarized plane electromagnetic wave in the interior electrodynamic problem will be called an ideal interior Huygens cube.

The problem of electromagnetic-wave scattering in the interior Huygens cube was simulated by means of the ANSYS HFSS v. 15 3D electrodynamic software package [7].

2. RESULTS OF SIMULATION OF THE INTERIOR HUYGENS CUBE

The simulation was performed in a frequency range from 1 to 300 GHz with a step of 1 GHz. The convergence in the absolute values of the elements of the

scattering matrix Delta S was 0.02, the total number of tetrahedra was 1956, the size of the resulting matrix was 10690, and the required storage was 49.3 MB. The total computation time on a PC with the Intel Core i7 processor with the frequency of 2.79 GHz and 12 GB RAM was 7 min 35 s.

The characteristics of the interior Huygens cube were calculated for the frequencies of 1 to 300 GHz. For example, at a frequency of 1 GHz, the side of this cube was 1/300 of the wavelength, which corresponds to the quasi-static case. Starting from a frequency of 30 GHz, which corresponds to the Huygens cube side of 1/10 of the wavelength, the static components are

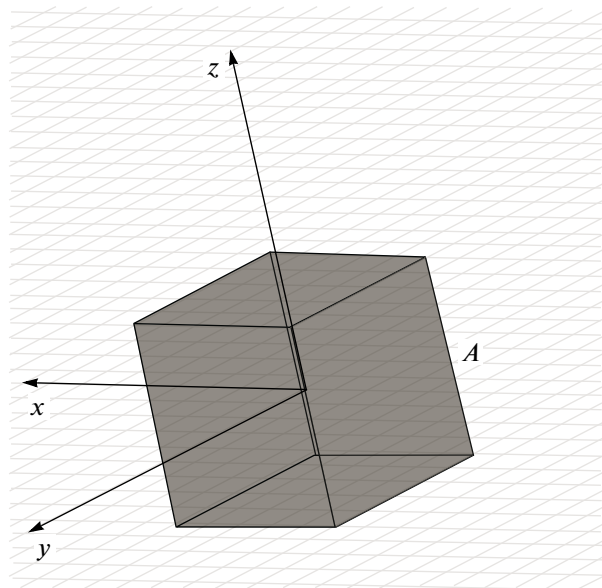


Fig. 1. Geometry of vacuum-filled cube A .

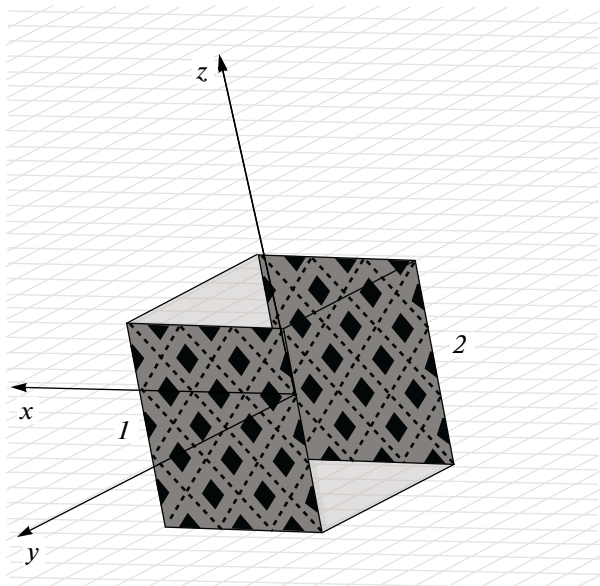


Fig. 2. Short-circuited faces 1 and 2 of cube *A*.

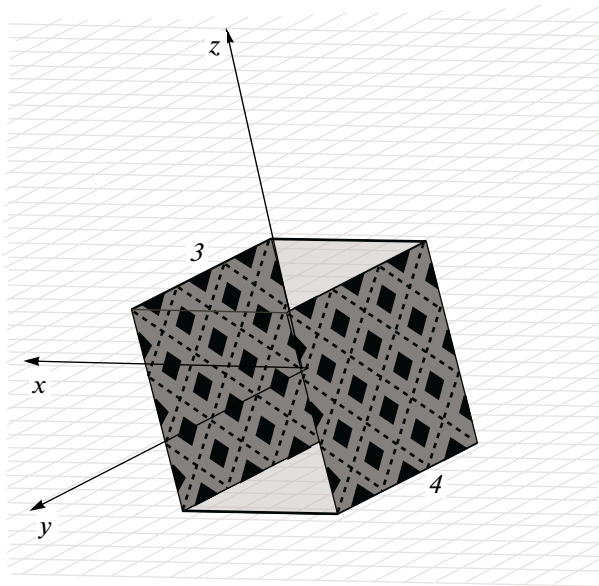


Fig. 3. Open-circuited faces 3 and 4 of cube *A*.

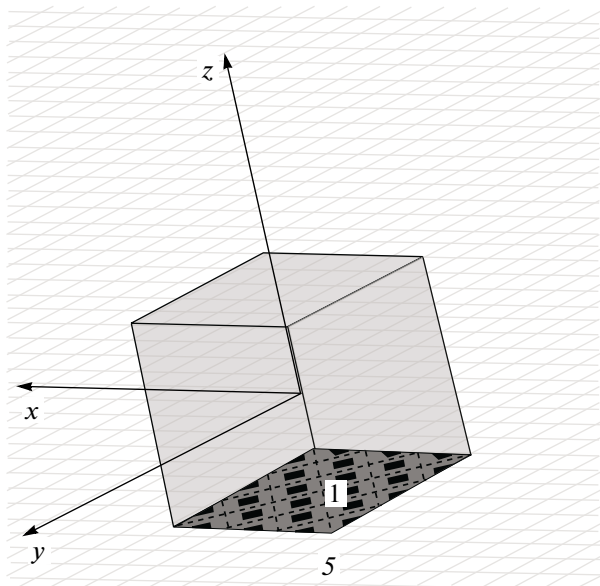


Fig. 4. Face 5 of cube *A*, on which the excitation and matching boundary condition is imposed.

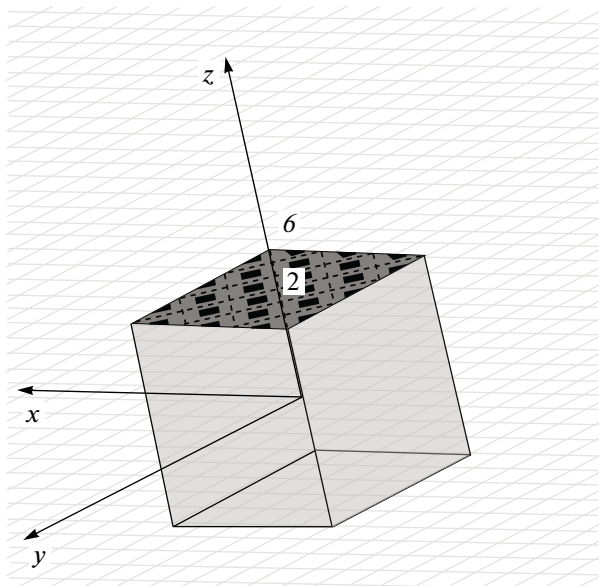


Fig. 5. Face 6 of cube *A*, on which the excitation and matching boundary condition is imposed.

not sufficient for describing the phenomena inside the cube. For the SWR presented in Fig. 9, up to 30 GHz (less than $1/10$ of the wavelength), the SWR does not exceed 1.00001. Figure 10 shows the frequency reflection characteristic for the interior Huygens cube, from which we see that, up to the frequency of 30 GHz, the reflectance is below -140 dB. With a further increase in the frequency, above 150 GHz (which corresponds to the value exceeding half a wavelength), the SWR slightly increases. As we see from Figs. 9 and 10, the

increase in the SWR is small and does not exceed -58 dB. The loss is very small. Its extremum is at the frequency 270 GHz and does not exceed -0.000055 dB, as is evident from Fig. 11, which shows the frequency attenuation characteristic for the interior Huygens cube. The obtained frequency characteristics indicate a reduction in the accuracy of computation in the amplitude with an increase in the frequency. Since, for the exact solution, $SWR = 1$, the loss is zero in the entire frequency range. This is the result of the numer-

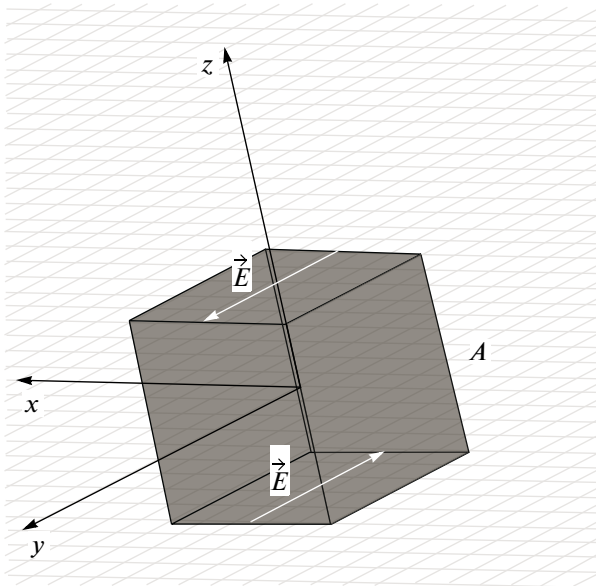


Fig. 6. Directions of the electric field vectors \vec{E} of the waves incident onto faces 5 and 6 of cube A .

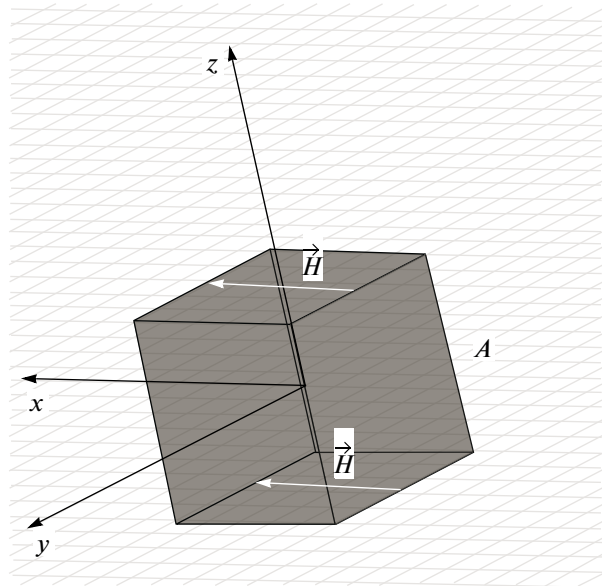


Fig. 7. Directions of the magnetic field vectors \vec{H} of the waves incident onto faces 5 and 6 of cube A .

ical solution for the amplitude obtained with the use of the ANSYS HFSS v. 15 code.

The frequency characteristic of phase φ of the transmission coefficient is presented in Fig. 12. It should be noted that the phase of the transmission coefficient should be reduced by 180° , because the ANSYS HFSS v. 15 code for the polarization of the electric field on faces 5 and 6 chooses the same direction, whereas these faces are situated on the opposite sides of the cube. Then, this modified characteristic can be used for constructing the frequency characteristic of the time delay, which is shown in Fig. 13. This characteristic is constructed from the following formula:

$$\Delta t = \frac{\arg S_{12} - \pi}{2\pi f}, \quad (1)$$

where Δt is the delay in seconds, $\arg S_{12}$ is the phase of the transmission coefficient calculated by the ANSYS HFSS v. 15 code in radians, and f is the frequency in hertz.

As we see from Fig. 13, the delay t of a signal passing through the interior Huygens cube is practically independent of frequency and is rather close to its exact value of 3.33(3) ps. For a more accurate description of the frequency behavior of the signal delay, Fig. 14 shows the frequency dependence of the relative deviation of delay t_0 of a signal passing through the interior Huygens cube from the exact value. As is evident from Fig. 14, the relative error of the computation performed with the use of the ANSYS HFSS v. 15 code with a chosen accuracy is less than 3×10^{-11} at a frequency of 1 GHz and increases to 0.0005 at a fre-

quency of 300 GHz. The curve of the frequency dependence of the relative phase error resembles an parabola.

Thus, with an increase in frequency, the error of computation for the interior Huygens cube performed with the use of the ANSYS HFSS v. 15 code increases in the amplitude and in the phase.

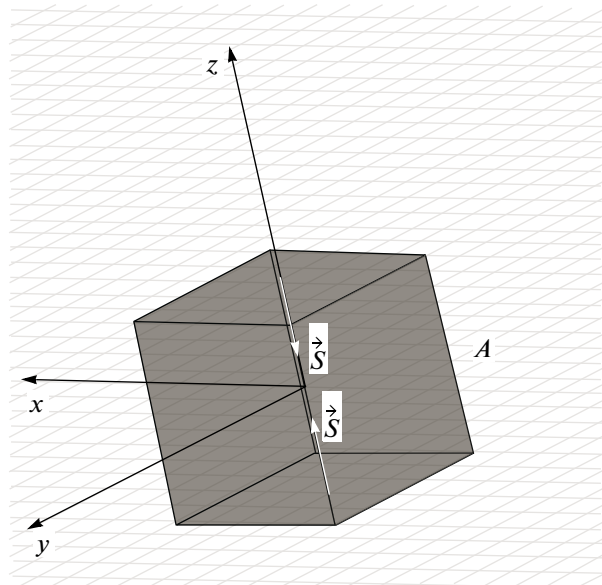


Fig. 8. Directions of the electromagnetic energy flux densities (Poynting vectors) \vec{S} of the waves incident onto faces 5 and 6 of cube A .

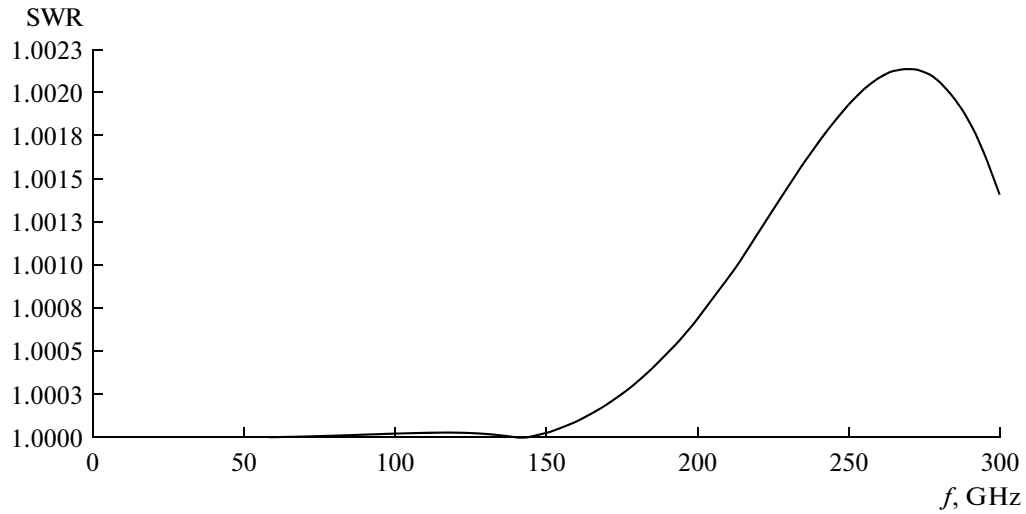


Fig. 9. Frequency characteristic of the SWR for the interior Huygens cube.

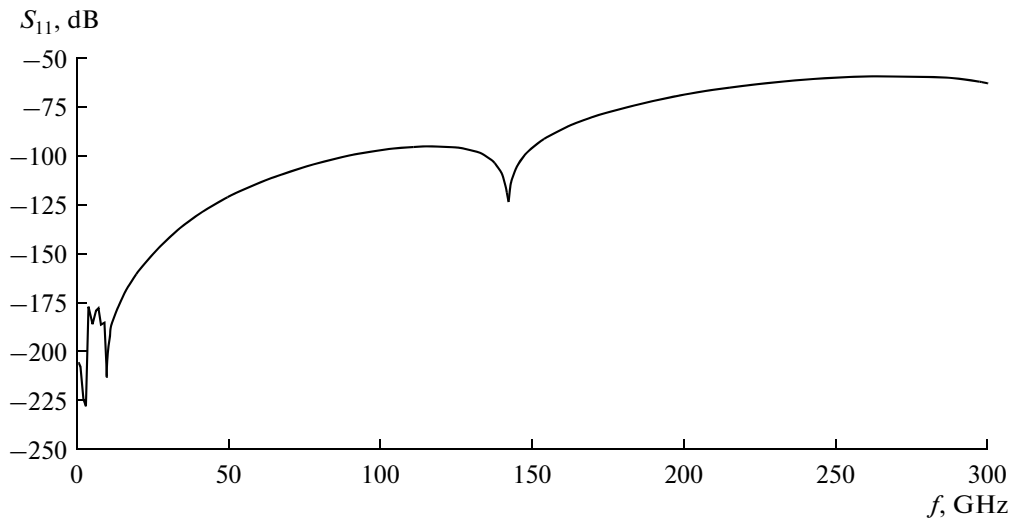


Fig. 10. Frequency characteristic of reflection coefficient S_{11} of the interior Huygens cube.

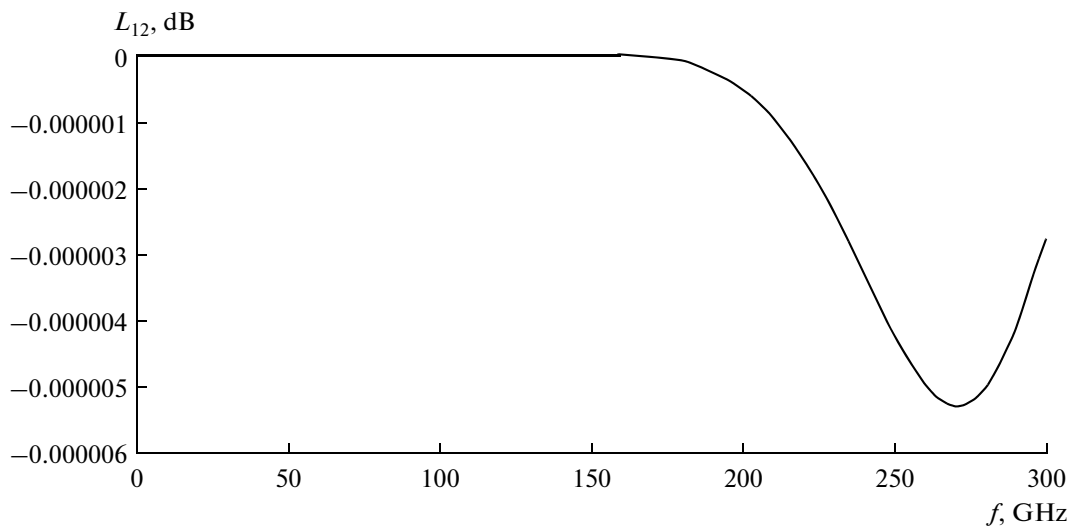


Fig. 11. Frequency characteristic of attenuation L_{12} for the interior Huygens cube.

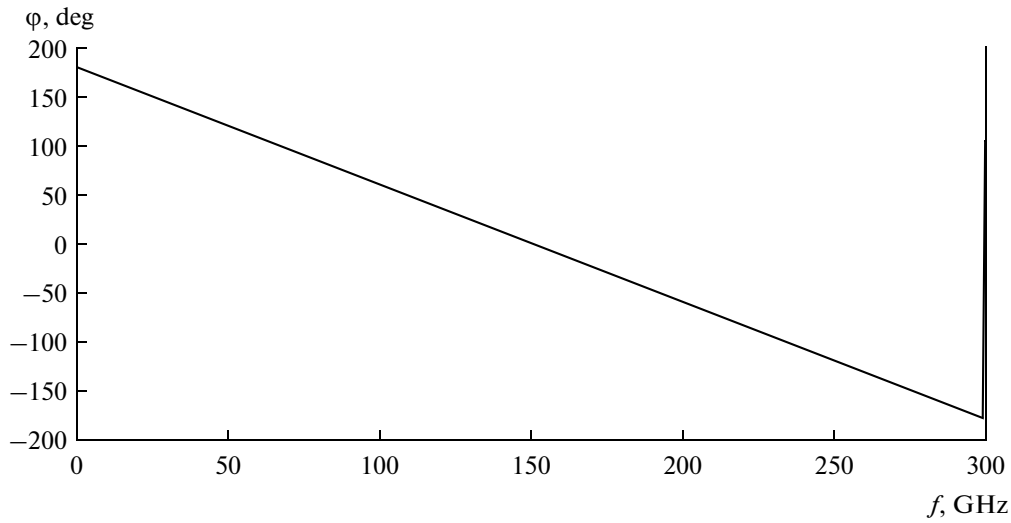


Fig. 12. Frequency characteristic of phase φ of the transmission coefficient for the interior Huygens cube.

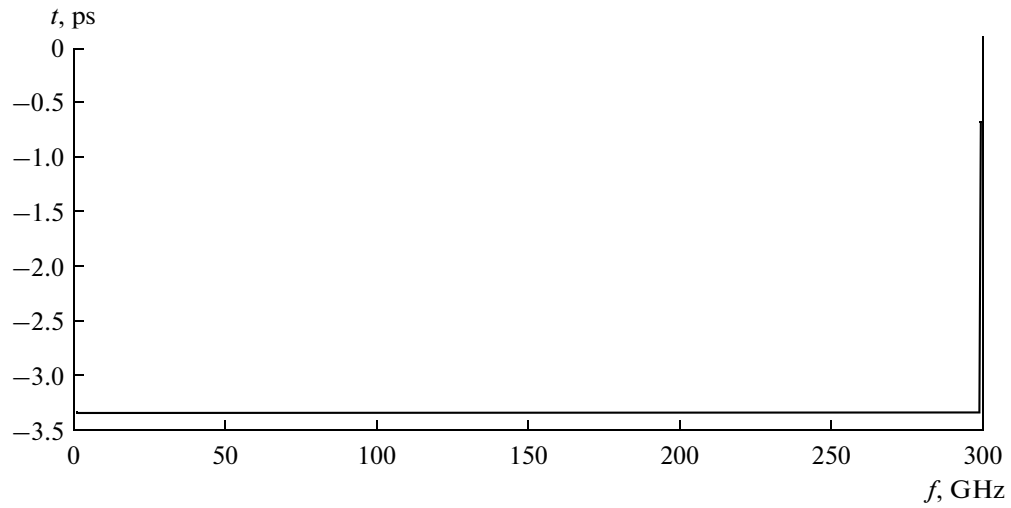


Fig. 13. Frequency characteristic of transmission delay t for the interior Huygens cube.

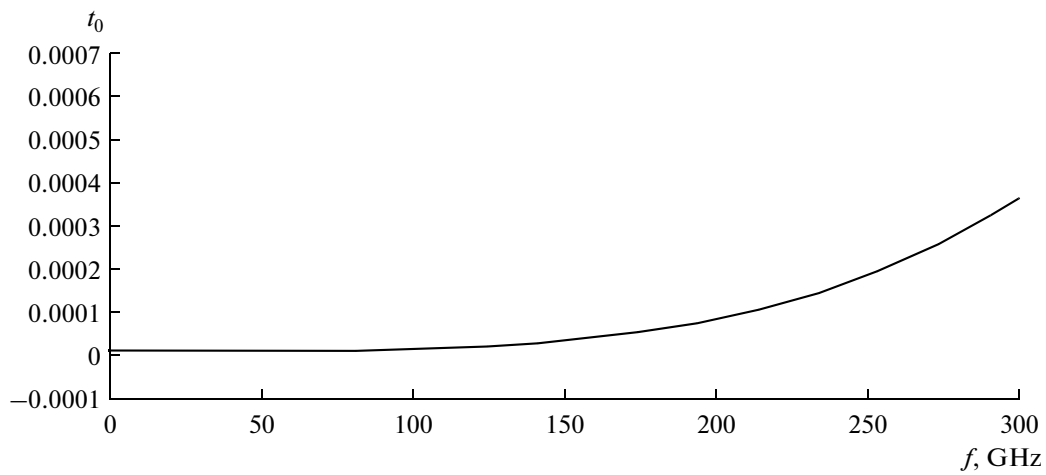


Fig. 14. Frequency characteristic of the relative error in the signal transmission delay t_0 for the interior Huygens cube.

CONCLUSIONS

We have numerically simulated the problem of the transmission of a plane electromagnetic wave through the interior Huygens cube, which is a Floquet channel [8]. It should be noted that a travelling plane wave is characterized by two parameters: the amplitude and the phase. We should dwell on the accuracy of the numerical solution for the amplitude and phase obtained with the use of the ANSYS HFSS v. 15 code.

The accuracy of the numerical solution for the amplitude is the following:

(i) up to 15 GHz (1/20 of the wavelength), the error in the amplitude reflection coefficient is -170 dB, whereas the exact value is ∞ ;

(ii) from 15 GHz (1/20 of the wavelength) to 150 GHz (1/2 of the wavelength), the amplitude reflection coefficient decreases from -170 dB to -95 dB;

(iii) from 150 GHz (1/2 of the wavelength) to 300 GHz (1 wavelength), the amplitude reflection coefficient decreases from -95 dB to -59 dB.

From these data, we see that, with an increase in the frequency (reduction in the wavelength), the error in the amplitude increases.

The error of the numerical solution for the phase will be characterized by the relative delay of the signal from the exact value:

(i) up to 15 GHz (1/20 of the wavelength), the relative error in the delay does not exceed 5×10^{-9} ;

(ii) from 15 GHz (1/20 of the wavelength) to 150 GHz (1/2 of the wavelength), the relative error in the delay decreases from 5×10^{-9} to 4×10^{-5} ;

(iii) from 150 GHz (1/2 of the wavelength) to 300 GHz (1 wavelength), the relative error in the delay decreases from 4×10^{-5} to 4×10^{-4} .

From these data, we see that, with an increase in the frequency (reduction in the wavelength), the phase error also increases.

Thus, we have studied the accuracy of the numerical solution of the problem obtained with the use of

the ANSYS HFSS v. 15 code for both the amplitude and phase.

The solution of this class of problems for various input cross sections including circular, coaxial, and strip-line should be used in the numerical simulation of various devices. Such solutions serve for estimating the total methodic error of numerical simulation and, by analogy with the calibration of inputs in experimental studies, the results of such calculations of transmission lines of the corresponding inputs of multiport devices can be used for such calibration but with the use of numerical simulation.

REFERENCES

1. D. M. Sazonov, A. N. Gridin, and B. A. Mishustin, *Microwave Circuits* (Vysshaya Shkola, Moscow, 1981; Mir, Moscow, 1982).
2. K. N. Klimov, A. S. Godin, and V. V. Perfil'ev, *Schematics of Elementary Space Volume in Magnetized Plasma* (LAP Lambert Academic Publishing, Saarbrücken, Germany, 2012) [in Russian].
3. K. N. Klimov, V. V. Perfil'ev, and A. S. Godin, *Time-Domain Electrodynamics Analysis of Two-Dimensional Inhomogeneous Media* (LAP Lambert Academic Publishing, Saarbrücken, Germany, 2012) [in Russian].
4. G. T. Markov and A. M. Sazonov, *Antennas* (Energiya, Moscow, 1975) [in Russian].
5. A. S. Petrov and M. A. Zheksenov, "Scanning Antenna Array Concentrated in the Volume of a Physical Point," *J. Commun. Technol. Electron.* **59**, 241 (2014).
6. M. A. Zheksenov and A. S. Petrov, "An Adaptive Antenna Array Formed from an E3M3 Radiator," *J. Commun. Technol. Electron.* **59**, 710 (2014).
7. S. E. Bankov and A. A. Kurushin, "Designing of microwave devices and antennas with Ansoft HFSS," *J. Radioelectron.*, No. 5 (2009); <http://jre.cplire.ru/win/library/7/text.pdf>
8. S. I. Baskakov, *Fundamentals of Electromagnetics* (Sovetskoe Radio, Moscow, 1973) [in Russian].

Translated by E. Chernokozhin